

Severe acute respiratory syndrome coronavirus 3C-like protease-induced apoptosis

Cheng-Wen Lin^{1,2}, Kuan-Hsun Lin¹, Tsung-Han Hsieh¹, Shi-Yi Shiu¹ & Jeng-Yi Li¹

¹Department of Medical Laboratory Science and Biotechnology, China Medical University, Taichung, Taiwan and ²Clinical Virology Laboratory, Department of Laboratory Medicine, China Medical University Hospital, Taichung, Taiwan

Correspondence: Cheng-Wen Lin,
Department of Medical Laboratory Science
and Biotechnology, China Medical University,
No. 91, Hsueh-Shih Road, Taichung 404,
Taiwan. Tel.: 886 4 22062341; fax: +886 4
22057414; e-mail: cwlin@mail.cmu.edu.tw

Received 24 June 2005; accepted 6 October
2005.

First published online 17 January 2006.

doi:10.1111/j.1574-695X.2006.00045.x

Editor: Willem van Eden

Keywords

SARS-coronavirus; 3CL^{pro}; apoptosis; reactive
oxygen species; nuclear factor-kappa B
signalling.

Introduction

Severe acute respiratory syndrome (SARS), with high fever, malaise, headache, dry cough and generalized, interstitial infiltrates in the lung, is caused by a novel virus, SARS-associated coronavirus (SARS-CoV) (Lee *et al.*, 2003; Tsang *et al.*, 2003; Hsueh *et al.*, 2004). SARS-CoV is rapidly transmitted through aerosols, and caused 8447 reported cases with 811 deaths worldwide during a short period from February to June 2003 (Peiris *et al.*, 2003; Poutanen *et al.*, 2003). Around 20% of SARS cases developed an acute respiratory distress syndrome requiring mechanical ventilation. Pathological examination of the lung indicated that bronchial epithelial denudation, loss of cilia, multinucleated syncytial cells and squamous metaplasia were found in lung tissues of SARS patients (Lang *et al.*, 2003; Nicholls *et al.*, 2003). Abnormal laboratory findings in SARS patients included lymphopenia, leucopenia, thrombocytopenia and an increase in aminotransferase, lactate dehydrogenase, creatine kinase, interleukin-6 (IL-6) and IL-8 in serum (Wang *et al.*, 2004; Huang *et al.*, 2005).

SARS-CoV particles contain a single positive-stranded RNA genome that is approximately 30 kb in length and has a 5' cap structure and 3' polyA tract (Enjuanes *et al.*, 2000; Holmes, 2001; Lai & Holmes, 2001). The SARS-CoV

Abstract

The pathogenesis of severe acute respiratory syndrome-associated coronavirus (SARS-CoV) is an important issue for the treatment and prevention of severe acute respiratory syndrome. Recently, SARS-CoV has been demonstrated to induce cell apoptosis in Vero-E6 cells. The possible role of SARS-CoV 3C-like protease (3CL^{pro}) in virus-induced apoptosis is characterized in this study. Growth arrest and apoptosis via caspase-3 and caspase-9 activities were demonstrated in SARS-CoV 3CL^{pro}-expressing human promonocyte cells. The fluorescence intensity of dihydrorhodamine 123 staining indicated that cellular reactive oxygen species were markedly increased in SARS-CoV 3CL^{pro}-expressing cells. Moreover, *in vivo* signalling pathway assay indicated that 3CL^{pro} increased the activation of the nuclear factor-kappa B-dependent reporter, but inhibited activator protein-1-dependent transcription. This finding is likely to be responsible for virus-induced apoptotic signalling.

genome encodes for replicase, spike, envelope, membrane and nucleocapsid. The replicase gene encodes two large overlapping polypeptides (replicase 1a and 1ab, *c.* 450 and *c.* 750 kDa, respectively), including 3C-like protease (3CL^{pro}), RNA-dependent RNA polymerase and RNA helicase for viral replication and transcription (Ziebuhr *et al.*, 2000). SARS-CoV replicates in Vero-E6 cells with cytopathic effects (Ng *et al.*, 2003; Yan *et al.*, 2004), and also induces AKT signalling-mediated cell apoptosis (Mizutani *et al.*, 2004). Recently, the SARS-CoV nucleocapsid (SARS-CoV N) protein has been demonstrated to induce actin reorganization and apoptosis in COS-1 monkey kidney cells by down-regulating extracellular signal-regulated kinase (ERK) and up-regulating c-Jun N-terminal kinase (JNK) and p38 mitogen-activated protein kinase (MAPK) pathways (Surjit *et al.*, 2004). As the 3C protease of the picornaviruses poliovirus, enterovirus 71 and rhinovirus induces cell apoptosis (Li *et al.*, 2002; Calandria *et al.*, 2004; Funkhouser *et al.*, 2004), the possible role of SARS-CoV 3CL^{pro} in virus-induced apoptosis is of interest.

In this study, we investigated the effects of SARS-CoV 3CL^{pro} on cellular functions. The cell growth curve, annexin V staining, caspase-3 and caspase-9 activities, oxidative stress and *in vivo* signalling pathways were measured to determine the effects of SARS-CoV 3CL^{pro}-induced apoptosis.

Therefore, this study demonstrated the significance of SARS-CoV 3CL^{pro}-induced apoptosis.

Materials and methods

Cell culture and transfection

To examine the effect of SARS-CoV 3CL^{pro} in cells, the 3CL^{pro} gene was amplified using PCR and then cloned into the pcDNA3.1 vector, as described previously (Lin *et al.*, 2004b). The resulting plasmid pcDNA3.1-SARS-CoV 3CL^{pro} (pSARS-CoV 3CL^{pro}) (4.5 µg), plus indicator vector pEGFP-N1 (0.5 µg), was transfected into HL-CZ cells, a human promonocyte cell line (Liu *et al.*, 1991), using the GenePorter reagent. According to the manufacturer's instructions (Gene Therapy Systems, San Diego, CA), the transfected cells were maintained in 2 mL of RPMI 1640 medium containing 20% fetal bovine serum (FBS) after 5 h of incubation with a mixture of the plasmid DNA and GenePorter reagent. For the selection of the transfected cell clones, cells were incubated with RPMI 1640 medium containing 10% FBS and 800 µg mL⁻¹ of G418. Enhanced green fluorescent protein (EGFP) expression in transfected cells with pSARS-CoV 3CL^{pro} plus pEGFP-N1 was observed using immunofluorescence microscopy.

Immunofluorescence staining and Western blotting of 3CL^{pro}-expressing cells

The stably transfected cells were washed once in phosphate-buffered saline (PBS), and then fixed in ice – 10% methanol for 2 min. The cells were subsequently incubated with anti-His tag antibody for 1 h, followed by rhodamine-conjugated antimouse immunoglobulin G (IgG) antibody for 1 h. After washing three times in PBS, photographs of the cells were taken using immunofluorescence microscopy. For western blotting, the cell lysates were dissolved in 2× sodium dodecylsulphate-polyacrylamide gel electrophoresis (SDS-PAGE) sample buffer without 2-mercaptoethanol, and boiled for 10 min. Proteins were resolved on 12% SDS-PAGE gels and transferred to nitrocellulose paper. The resultant blots were blocked with 5% skimmed milk, and then incubated with the appropriately diluted anti-His tag monoclonal antibody (Serotec, Oxford, UK) for 3 h. The blots were then washed with 1× Tris-buffered saline Tween 20 (TBST) three times and overlaid with a 1 : 5000 dilution of goat antimouse IgG antibodies conjugated with alkaline phosphatase (PerkinElmer Life Sciences Inc., Boston, MA). Following 1 h of incubation at room temperature, the blots were developed with tetrazolium salt/5-bromo-4-chloro-3-iodolylphosphate (TNBT/BCIP) (Gibco, Invitrogen, Merelbeke, Belgium).

Annexin V staining for apoptosis detection

After washing with cold PBS, transfected cells were resuspended in annexin-binding buffer (10 mM HEPES, 140 mM NaCl and 2.5 mM CaCl₂, pH 7.4). Each 100 µL of cell suspension was incubated with 5 µL of antiannexin V antibody (Biocompare, Abcom, Cambridge, UK) at room temperature for 15 min. The apoptotic cells were further stained using a horseradish peroxidase/diaminobenzidine (HRP/DAB) system of the SuperPicTureTM Polymer Detection Kit (Zymed Laboratories Inc., San Francisco, CA). The percentage of apoptotic cells with a permanent intense brown deposit was counted at ×200 magnification using bright field microscopy.

Fluorimetric assay of caspase profiling

Transfected cells were harvested to measure the activity of caspase-2, -3, -8 and -9 using BD ApoAlert Caspase Fluorescent Assay Kits (BD Biosciences, Franklin Lakes, NJ); 2 × 10⁵ cells per well were lysed in 50 µL of lysis buffer and centrifuged at 12 000 g for 5 min at 4 °C. The supernatant was transferred into the well of the caspase profiling assay plate and incubated at 37 °C for 2 h. Finally, the caspase profiling assay plate was analysed in a fluorescent plate reader with excitation at 380 nm and emission at 460 nm.

Detection of reactive oxygen species

Reactive oxygen species (ROS) of the 3CL^{pro}-expressing cells were quantified by staining with dihydrorhodamine 123 (DHR, Molecular Probes, Invitrogen). After incubation with 20 µM DHR in RPMI 1640 medium for 15 min, the cells were washed three times with PBS, and the fluorescence intensity of the cells was measured with excitation at 492 nm and emission at 535 nm.

Transient transfections of cis-reporter plasmids for signalling pathway assay

The cis-reporter plasmids pSRE-Luc, pGAS-Luc, p53-Luc, pAP1-Luc and pNF-κB-Luc were purchased from the Stratagene Company (La Jolla, CA). The SARS-CoV 3CL^{pro}-expressing and mock cells were transfected with a cis-reporter plasmid using the GenePorter reagent. After 18 h of incubation, the luciferase activity in the indicated cells was measured using the dual Luciferase Reporter Assay System (Promega, Madison, WI) and the Luminometer TROPIX TR-717 (Applied Biosystems, Foster City, CA).

Results

Expression of SARS-CoV 3CL^{pro} in HL-CZ promonocyte cells

To examine the effect of SARS-CoV 3CL^{pro} on cell function, co-transfection of human promonocyte HL-CZ cells with

Fig. 1. Expression of severe acute respiratory syndrome-associated coronavirus 3C-like protease (SARS CoV 3CL^{Pro}) in human promonocyte HL-CZ cells. Transfected cells with pcDNA3.1 plus pEGFP-N1 (a, b) or pSARS CoV 3CL^{Pro} plus pEGFP-N1 (c, d) were selected using a 2-week incubation with G418. The green fluorescent protein (GFP) (a, c) and His-tag fusion protein (b, d) in the transfected cells were examined by fluorescence microscopy. The His-tag fusion protein was detected using immunofluorescence staining of anti-His tag antibody and rhodamine-conjugated antimouse IgG antibody.

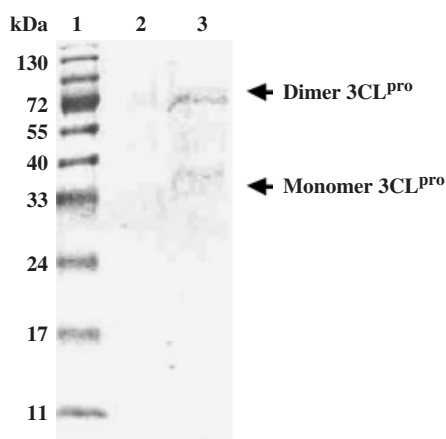
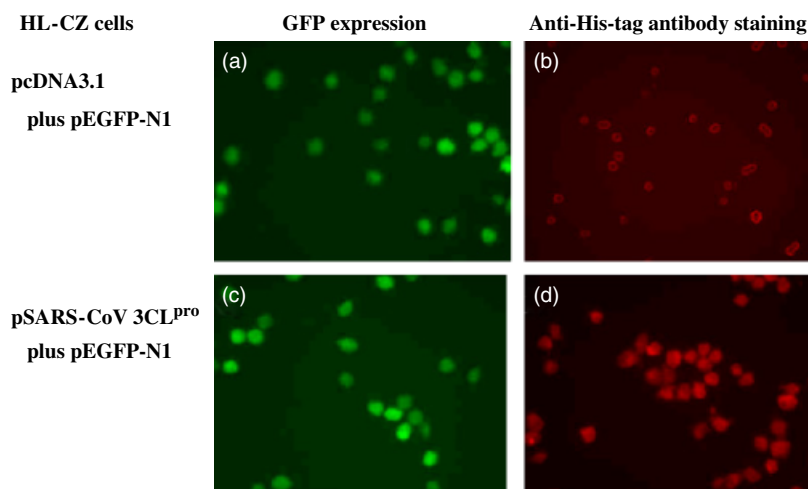


Fig. 2. Western blot assay of severe acute respiratory syndrome-associated coronavirus 3C-like protease (SARS-CoV 3CL^{Pro})-expressing cells with anti-His tag antibody. The cell lysates from stably transfected cells with pcDNA3.1 (lane 2) and pSARS-CoV 3CL^{Pro} (lane 3) were analysed by 10% sodium dodecylsulphate-polyacrylamide gel electrophoresis and electrophoretically transferred to nitrocellulose paper. The blot was probed with mouse anti-His tag antibodies, and developed with an alkaline phosphatase-conjugated secondary antibody and tetrazolium salt/5-bromo-4-chloro-3-idolylphosphate (NBT/BCIP) substrates. Lane 1 was the molecular marker. kDa, kilodaltons.

the recombinant plasmid pSARS-CoV 3CL^{Pro} and a green fluorescent protein (GFP) reporter was carried out (Fig. 1). Immunofluorescent staining of transfected cells with anti-His tag antibody revealed that the 3CL^{Pro} His-tag fusion protein localized predominantly in the cytoplasm and nucleus (Fig. 1d), in contrast with mock cells expressing the His-tag only (Fig. 1b). Western blotting analysis of cell lysates with anti-His tag antibody showed that a major 68 kDa band for the dimer and a minor 34 kDa band for the monomer were observed in cells transfected with pSARS-CoV 3CL^{Pro} (Fig. 2, lane 3), but not in mock cells

(Fig. 2, lane 2). This result demonstrates the functional expression of SARS-CoV 3CL^{Pro} in HL-CZ cells.

Cellular effect of SARS-CoV 3CL^{Pro} in promonocyte cells

To further analyse the cellular effect of SARS-CoV 3CL^{Pro}, the growth curves of 3CL^{Pro}-expressing cells and mock cells were obtained by direct counting assay (Fig. 3a). The cell growth curve of 3CL^{Pro}-expressing cells increased more slowly than that of mock cells. This result demonstrates a significant inhibitory effect of SARS-CoV 3CL^{Pro} on the growth of human promonocyte cells. In addition, annexin V staining indicated a significant difference in the percentage of apoptotic cells between 3CL^{Pro}-expressing cells (20%) and mock cells (3%) (Figs 3b and c). SARS-CoV 3CL^{Pro}-induced apoptosis was also measured with a fluorimetric caspase profiling assay (Figs 4a and b). Caspase-3 activity in 3CL^{Pro}-expressing cells was 3.04-fold greater than that in the presence of the caspase-3 inhibitor and 2.1-fold greater than that in mock cells (Fig. 4a). Caspase-9 activity in 3CL^{Pro}-expressing cells was about 1.3-fold greater than that in mock cells and in the presence of the caspase-9 inhibitor (Fig. 4b). The activities of caspase-2 and caspase-8 were also determined, but no significant difference was found between 3CL^{Pro}-expressing cells and mock cells (data not shown).

Increase in ROS and activation of nuclear factor-kappa B signalling pathway by SARS-CoV 3CL^{Pro}

To test the possible mechanism of 3CL^{Pro}-induced apoptosis, ROS production and the *in vivo* signal transduction pathway in SARS-CoV 3CL^{Pro}-expressing cells were investigated (Figs 5 and 6). DHR staining was carried out for ROS detection. A significant increase in ROS was measured in 3CL^{Pro}-expressing cells (2.3-fold higher) relative to pcDNA3.1-expressing cells (Fig. 5). To measure signal

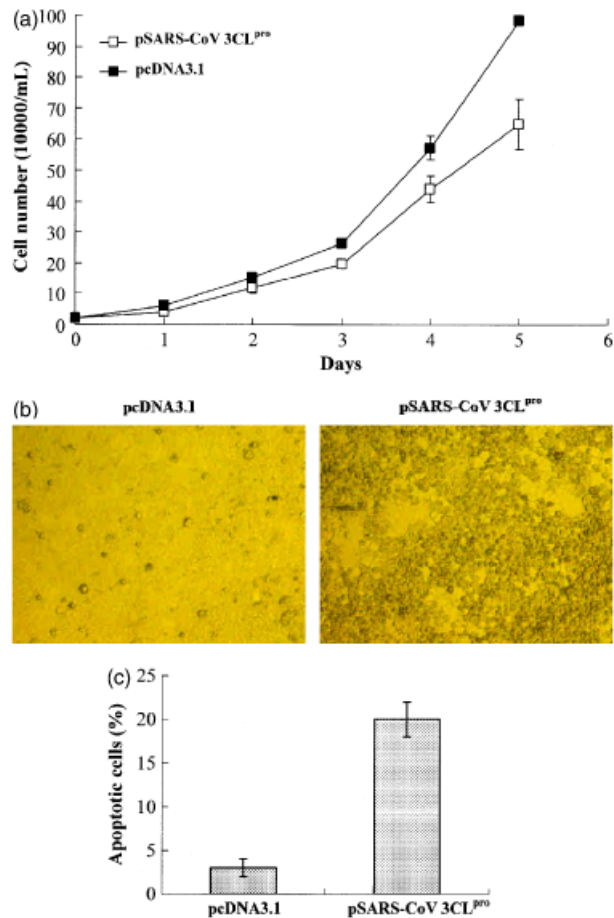


Fig. 3. The cellular effect of severe acute respiratory syndrome-associated coronavirus 3C-like protease (SARS-CoV 3CL^{PRO}) in HL-CZ cells. (a) Growth curve of SARS-CoV 3CL^{PRO}-expressing cells compared with mock cells. Transfected cells with pcDNA3.1 or pSARS-CoV 3CL^{PRO} were cultured in 25 cm² flasks at a density of 10 000 cells mL⁻¹ in RPMI medium with 10% fetal bovine serum (FBS) and 800 µg mL⁻¹ G418. Cells in duplicate flasks were harvested and counted manually each day. (b) Apoptosis of HL-CZ cells with pcDNA3.1 or pSARS-CoV 3CL^{PRO} was detected using annexin V staining. After washing with phosphate-buffered saline (PBS), transfected cells were resuspended in annexin-binding buffer with 5 µL of antiannexin V antibody. The apoptotic cells were stained using a horseradish peroxidase/diaminobenzidine (HRP/DAB) system. (c) The percentage of apoptotic cells with a permanent intense brown deposit was counted at $\times 200$ magnification using bright field microscopy.

transductions, transient transfection of 3CL^{PRO}-expressing cells and mock cells with a cis-reporter plasmid was subsequently performed to detect the *in vivo* signal transduction pathway (Fig. 6). The luciferase activity of cis-reporter plasmids indicated that SARS-CoV 3CL^{PRO} activated the expression of a nuclear factor-kappa B (NF- κ B)-dependent reporter gene in HL-CZ cells (2.15-fold increase), but inhibited activator protein-1 (AP1)-dependent transcription (0.45-fold decrease) (Fig. 6). In addition, no significant

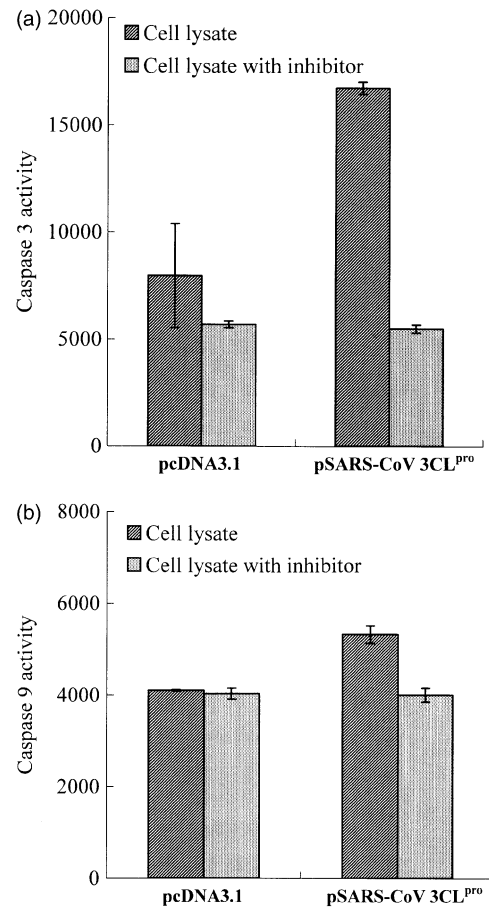


Fig. 4. Fluorimetric caspase-3 (a) and caspase-9 (b) activity assay in severe acute respiratory syndrome-associated coronavirus 3C-like protease (SARS-CoV 3CL^{PRO})-expressing HL-CZ cells. Cells (2×10^5) were lysed in 50 µL of lysis buffer and centrifuged at 12 000 *g* for 5 min at 4 °C. The supernatant was transferred into the well of a BD ApoAlert Caspase Fluorescent Assay Kit assay plate. After incubation at 37 °C for 2 h, the caspase profiling assay plate was analysed in a fluorescent plate reader with excitation at 380 nm and emission at 460 nm.

effect on interferon-stimulated response element (ISRE)- and interferon-gamma-activated site (GAS)-dependent transcriptions was induced by SARS-CoV 3CL^{PRO}.

Discussion

A mixture of the active dimer form and the inactive monomer form of SARS-CoV 3CL^{PRO} was generated in human promonocyte HL-CZ cells (Fig. 2), consistent with bacterial expression systems (Fan *et al.*, 2004; Lin *et al.*, 2004b). Interestingly, the dimer was the major 3CL^{PRO} in HL-CZ cells, different from that in *Escherichia coli*-synthesized HL-CZ cells, where it was the monomer (Fan *et al.*, 2004; Lin *et al.*, 2004b). SARS-CoV 3CL^{PRO} influenced cell growth and induced apoptosis (Figs 3 and 4). Activation of caspase-3 and caspase-9, but not caspase-2 and caspase-8,

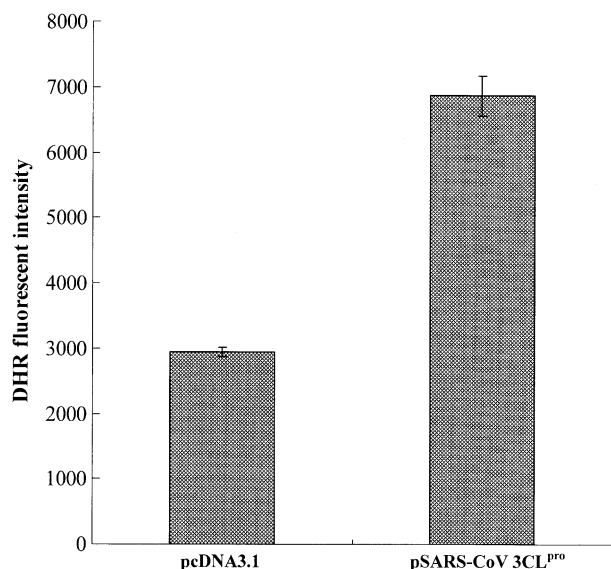


Fig. 5. Reactive oxygen species production of transfected cells using dihydrorhodamine 123 (DHR) staining. Cells were incubated with 20 μ M DHR in RPMI 1640 medium for 15 min. After washing three times with phosphate-buffered saline, the fluorescence intensity of the cells was measured with excitation at 492 nm and emission at 535 nm.

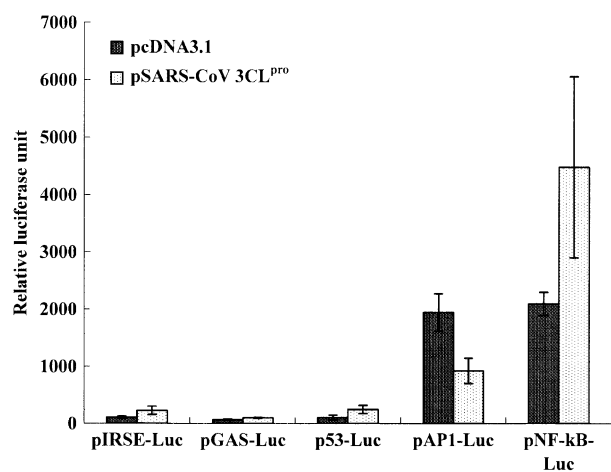


Fig. 6. Effect of *in vivo* signal transduction pathway in severe acute respiratory syndrome-associated coronavirus 3C-like protease (SARS-CoV 3CL^{pro})-expressing cells on the cis-reporter systems of interferon-stimulated response element (ISRE), interferon-gamma-activated site (GAS), p53, activator protein-1 (AP1) and nuclear factor-kappa B (NF- κ B). SARS-CoV 3CL^{pro}-expressing cells and mock cells were transiently transfected with the cis-reporter plasmids pISRE-Luc, pGAS-Luc, p53-Luc, pAPI-Luc and pNF- κ B, respectively. The indicated promoter activity was measured using a luciferase assay.

was correlated with SARS-CoV 3CL^{pro}-induced apoptosis in HL-CZ cells (Fig. 4). A similar caspase activity profile has been reported in poliovirus 3C-induced apoptosis via caspase-3 activation (Calandria *et al.*, 2004).

SARS-CoV 3CL^{pro} caused a significant increase in ROS production in HL-CZ cells (Fig. 5) which, in turn, were involved in 3CL^{pro}-induced apoptosis. Recently, ROS-mediated apoptosis has also been reported in viral infections, such as Japanese encephalitis virus (Lin *et al.*, 2004a) and influenza virus (Uchide *et al.*, 2002). *In vivo* signalling pathway assay indicated that 3CL^{pro} increased the activation of the NF- κ B-dependent reporter, but inhibited AP1-dependent transcription (Fig. 6). This finding indicates that NF- κ B, but not c-Jun, is involved in 3CL^{pro}-induced apoptosis of human promonocyte cells. The transcription factor NF- κ B is produced in response to oxidative stress, being widely proposed to be involved in the mediation or prevention of apoptosis, and ROS serve as second messengers in the induction of the transcription factor NF- κ B (Bonizzi *et al.*, 1999). The activation of an NF- κ B-dependent reporter gene induced by SARS-CoV 3CL^{pro} (Fig. 6) was correlated with an increase in ROS production in HL-CZ cells. Consensus NF- κ B sites exist in the promoters of apoptosis-related genes and proinflammatory genes (Chen *et al.*, 2001), such as transforming growth factor- β (TGF- β), tumour necrosis factor- α (TNF- α), IL-1 α , IL-6 and IL-8. Interestingly, TGF- β , IL-6 and IL-8 are greatly increased in the acute phase sera of SARS patients (Huang *et al.*, 2005). Therefore, the activation of the NF- κ B signal transduction pathway induced by SARS-CoV 3CL^{pro} could be useful for elucidating the pathogenesis of SARS.

In conclusion, the cellular effects of SARS-CoV 3CL^{pro} in human promonocyte cells, such as growth arrest and apoptosis via caspase-3 and caspase-9 activities, have been well characterized in this study. ROS production and NF- κ B signalling are likely to be associated with SARS-CoV 3CL^{pro}-induced pathology.

Acknowledgement

We would like to thank the National Science Council (Taiwan) and China Medical University for financial support (NSC93-2320-B-039-051, 93-2745-B-039-004-URD and CMU-93-MT-04).

References

- Bonizzi G, Piette J, Schoonbroodt S, Greimers R, Havard L, Merville MP & Bours V (1999) Reactive oxygen intermediate-dependent NF-kappaB activation by interleukin-1beta requires 5-lipoxygenase or NADPH oxidase activity. *Mol Cell Biol* **19**: 1950–1960.
- Calandria C, Irurzun A, Barco A & Carrasco L (2004) Individual expression of poliovirus 2Apro and 3Cpro induces activation of caspase-3 and PARP cleavage in HeLa cells. *Virus Res* **104**: 39–49.

- Chen F, Castranova V & Shi X (2001) New insights into the role of nuclear factor-kappaB in cell growth regulation. *Am J Pathol* **159**: 387–397.
- Enjuanes L, Brian D, Cavanagh D, et al. (2000) Coronaviridae. *Virus Taxonomy* (van Regenmortel MHV, Fauquet CM, Bishop DHL, Carstens EB, Estes MK, Lemon SM, Mayo MA, McGeoch DJ, Pringle CR & Wickner RB, eds), pp. 835–849. Academic Press, New York.
- Fan K, Wei P, Feng Q, et al. (2004) Biosynthesis, purification, and substrate specificity of severe acute respiratory syndrome coronavirus 3C-like proteinase. *J Biol Chem* **279**: 1637–1642.
- Funkhouser AW, Kang JA, Tan A, Li J, Zhou L, Abe MK, Solway J & Hershenson MB (2004) Rhinovirus 16 3C protease induces interleukin-8 and granulocyte-macrophage colony-stimulating factor expression in human bronchial epithelial cells. *Pediatr Res* **55**: 13–18.
- Holmes KV (2001) Coronaviruses. *Fields Virology* (Knipe DM & Howley PM, eds), pp. 1187–1203. Lippincott Williams and Wilkins, New York.
- Hsueh PR, Chen PJ, Hsiao CH, et al. (2004) Patient data, early SARS epidemic, Taiwan. *Emerg Infect Dis* **10**: 489–493.
- Huang KJ, Su IJ, Theron M, Wu YC, Lai SK, Liu CC & Lei HY (2005) An interferon-gamma-related cytokine storm in SARS patients. *J Med Virol* **75**: 185–194.
- Lai MMC & Holmes KV (2001) Coronaviridae: the viruses and their replication. *Fields Virology* (Knipe DM & Howley PM, eds), pp. 1163–1185. Lippincott Williams and Wilkins, New York.
- Lang Z, Zhang L, Zhang S, Meng X, Li J, Song C, Sun L & Zhou Y (2003) Pathological study on severe acute respiratory syndrome. *China Med J (England)* **116**: 976–980.
- Lee N, Hui D, Wu A, et al. (2003) Lung pathology of fatal severe acute respiratory syndrome. *N Engl J Med* **348**: 1986–1994.
- Li ML, Hsu TA, Chen TC, Chang SC, Lee JC, Chen CC, Stollar V & Shih SR (2002) The 3C protease activity of enterovirus 71 induces human neural cell apoptosis. *Virology* **293**: 386–395.
- Lin RJ, Liao CL & Lin YL (2004a) Replication-incompetent virions of Japanese encephalitis virus trigger neuronal cell death by oxidative stress in a culture system. *J Gen Virol* **85**: 521–533.
- Lin CW, Tsai CH, Tsai FJ, Chen PJ, Lai CC, Wan L, Chiu HH & Lin KH (2004b) Characterization of trans- and cis-cleavage activity of the SARS coronavirus 3CLpro protease: basis for the in vitro screening of anti-SARS drugs. *FEBS Lett* **574**: 131–137.
- Liu WT, Chen CL, Lee SS, Chan CC, Lo FL & Ko YC (1991) Isolation of dengue virus with a human promonocyte cell line. *Am J Trop Med Hyg* **44**: 494–499.
- Mizutani T, Fukushi S, Saijo M, Kurane I & Morikawa S (2004) Importance of Akt signaling pathway for apoptosis in SARS-CoV-infected Vero E6 cells. *Virology* **327**: 169–174.
- Ng ML, Tan SH, See EE, Ooi EE & Ling AE (2003) Proliferative growth of SARS coronavirus in Vero E6 cells. *J Gen Virol* **84**: 3291–3303.
- Nicholls JM, Poon LL, Lee KC, et al. (2003) Lung pathology of fatal severe acute respiratory syndrome. *Lancet* **361**: 1773–1778.
- Peiris JS, Chu CM, Cheng VC, et al. (2003) Clinical progression and viral load in a community outbreak of coronavirus-associated SARS pneumonia: a prospective study. *Lancet* **361**: 1767–1772.
- Poutanen SM, Low DE, Henry B, et al. (2003) Identification of severe acute respiratory syndrome in Canada. *N Engl J Med* **348**: 1995–2005.
- Surjit M, Liu B, Jameel S, Chow VT & Lal SK (2004) The SARS coronavirus nucleocapsid protein induces actin reorganization and apoptosis in COS-1 cells in the absence of growth factors. *Biochem J* **383**: 13–18.
- Tsang KW, Ho PL, Ooi GC, et al. (2003) A cluster of cases of severe acute respiratory syndrome in Hong Kong. *N Engl J Med* **348**: 1977–1985.
- Uchida N, Ohyama K, Bessho T, Yuan B & Yamakawa T (2002) Effect of antioxidants on apoptosis induced by influenza virus infection: inhibition of viral gene replication and transcription with pyrrolidine dithiocarbamate. *Antiviral Res* **56**: 207–217.
- Wang WK, Chen SY, Liu IJ, et al. (2004) Temporal relationship of viral load, ribavirin, interleukin (IL)-6, IL-8, and clinical progression in patients with severe acute respiratory syndrome. *Clin Infect Dis* **39**: 1071–1075.
- Yan H, Xiao G, Zhang J, Hu Y, Yuan F, Cole DK, Zheng C & Gao GF (2004) SARS coronavirus induces apoptosis in Vero E6 cells. *J Med Virol* **73**: 323–331.
- Ziebuhr J, Snijder EJ & Gorbalenya AE (2000) Virus-encoded proteinases and proteolytic processing in the Nidovirales. *J Gen Virol* **81**: 853–879.